PTEP

Prog. Theor. Exp. Phys. **2022** 033B11(14 pages)
DOI: 10.1093/ptep/ptac040

Low-energy probes of the small cosmic microwave background amplitude in models of the radiative Higgs mechanism

Sunghoon Jung[1,2] and Kiyoharu Kawana[1,*]

[1] *Center for Theoretical Physics, Department of Physics and Astronomy, Seoul National University, Seoul 08826, Korea*
[2] *Astronomy Research Center, Seoul National University, Seoul 08826, Korea*
*E-mail: kiyoharukawana@gmail.com

Received November 9, 2021; Revised February 28, 2022; Accepted March 4, 2022; Published March 8, 2022

The small cosmic microwave background (CMB) amplitude $A_s \simeq 10^{-9}$ (or small temperature fluctuation $\delta T/T \simeq 10^{-5}$) typically requires an unnaturally small effective coupling of an inflaton $\lambda_\phi \sim 10^{-14}$. In models with non-minimal coupling ξ, extra suppression of the amplitude, e.g. by the inflaton's large field values, usually allows λ_ϕ to be much larger, but at the price of $\xi \gg 1$. Although the difficulties have not been strictly quantified, models with $\lambda_\phi \ll 1$ or $\xi \gg 1$ are harder to build. We show that the absence of new physics signals at TeV scale can suggest a relatively small $\xi \lesssim \mathcal{O}(1\text{–}100)$ with $\lambda_\phi \lesssim \mathcal{O}(10^{-4}\text{–}10^{-8})$, while constraining larger ξ with larger λ_ϕ more strongly. Above all, this is possible by a connection between low- and high-energy physics that can be made in scenarios where the $U(1)_X$ Higgs is an inflaton at a high scale while its renormalization running also induces the Coleman–Weinberg mechanism for the electroweak symmetry breaking at a low scale. The best TeV-scale signals are Z' resonances and Higgs signal strengths. We further find the connection particularly useful since the Z' mass is upper bounded in order to produce the correct A_s and the weak scale simultaenously. Utilizing the intriguing upper bounds, we work out the prospects for LHC 13 and 100 TeV pp colliders probing the parameter space of the small CMB amplitude in such a model.

Subject Index B32, B40, B72, B73, E63

1. Introduction

Although slow-roll is almost an inevitable requirement of inflation, the observed small temperature fluctuation in the universe (or, more precisely the small cosmic microwave background (CMB) amplitude) is not. Slow-roll inflation could have explained homogeneity, causality, and the quantum origin of density perturbations without predicting the small CMB amplitude. The observed $\delta T/T \sim 10^{-5}$ (or $A_s \sim 10^{-9}$) [1,2] is typically translated to $\lambda_\phi \sim 10^{-14} \ll 1$ for an effective quartic potential description $V = \lambda_\phi \phi^4/4$ of an inflaton ϕ. Such a small coupling is seemingly unnatural even though it is not a necessary prediction of slow-roll. Why is our universe realized so? Could this small CMB amplitude be related to other physics?

Anthropically, it has been argued that if $\delta T/T$ were larger too many black holes would have formed, while if smaller there would have been too little structure within the age of the universe [3]. It has even been argued that smaller $\delta T/T$ is more likely realized since it usually requires a flatter inflaton potential, inducing longer inflation and exponentially more Hubble patches [4].

Funded by SCOAP[3]

Higgs inflation has shed some light in this regard. The measured Higgs boson mass (combined with the top quark mass) surprisingly implies an almost vanishing Higgs potential near the Planck scale [5–9], via the renormalization group (RG) evolution in the Standard Model (SM). This not only made the electroweak vacuum possibly metastable, but also made the case for the Higgs boson as an inflaton [10–13] more plausible. As the first derivative of the Higgs potential is also expected to vanish near the same scale, some of the slow-roll conditions as well as the small potential height are automatically satisfied. Although Higgs inflation in its minimal form in the SM is not completely successful (so is generalized with an approximate inflection point [14–18], or a non-minimal coupling ξ [19–28], or various other features [29–33]), it became apparent that the small CMB amplitude may have some connections with other physics at distant energy scales.

Further, attempts were made to explain this interesting coincidence between high- and low-energy potential shapes by the multiple point principle [34–44] (i.e. why we seem to have almost degenerate minima at the electroweak and Planck scales) or by classical conformal invariance at the Planck scale (i.e. why the dimensionful Higgs quadratic term almost vanishes there). These hypotheses triggered the possibility of all the dimensionful parameters in the SM being induced by RG evolutions. In particular, electroweak symmetry breaking (EWSB) was successfully induced even starting from a vanishing Higgs potential (all potential terms vanish at the Planck scale) just with an additional $U(1)$ gauge symmetry, a charged fermion, and a symmetry-breaking scalar [45,46]. Also, it was shown that RG evolution can be used to realize (saddle-point) inflation together with the spontaneous symmetry breaking of $U(1)_{B-L}$ at a low scale [16–18,47]. In other words, models that can realize the Coleman–Weinberg mechanism with the assumption of an (almost) vanishing scalar potential at the Planck scale are compatible with inflation because they naturally predict a flat potential at high-energy scales.

Along this line, we study whether the small CMB amplitude can have meaningful connections or correlations with low-energy physics in the models where the ϕ inflaton's renormalization running induces both slow-roll inflation and radiative breaking of the electroweak symmetry (the Coleman–Weinberg (CW) mechanism). These well-measured high- and low-energy physics may induce non-trivial constraints on ϕ through perturbative quantum corrections (RG evolutions). See also Refs. [48–50] for similar directions where the connections between inflation predictions and low-energy (collider) observables were discussed. One of the novelties of our study is utilizing the maximum Z' mass allowed by the CW mechanism (see Section 4 for the details). In Section 2 we start by introducing our model and describing the CW mechanism, then in Section 3 we match this model to simple inflation models, and in Section 4 we interpret low-energy searches to the constraints on the parameter space of the inflation sector that can explain the small CMB amplitude.

2. The Coleman–Weinberg mechanism with $U(1)_X$

Our model consists of the CW mechanism for EWSB with vanishing dimensionful parameters at $M_{\rm Pl}$. This may represent one class of resolutions to the Planck–weak hierarchy problem.

The CW mechanism is realized with an additional $U(1)_X$, a linear combination of $U(1)_{B-L}$ and $U(1)_Y$ hypercharge, parameterized by x as

$$X = (B - L) - xY. \tag{1}$$

This model in our framework was worked out in Ref. [45] (including RG equations), with two small but necessary changes discussed below. To summarize, one generation (for simplicity) of right-handed neutrino ν_R and the SM-singlet scalar Φ with $X(\Phi) = 2$ are introduced, having Yukawa interactions

$$\mathcal{L} \ni -y_\nu \bar{\ell} \nu_R H - y_N \overline{(\nu_R)^c} \nu_R \Phi \tag{2}$$

and scalar potentials and the portal mixing

$$V = m_H^2 |H|^2 + m_\Phi^2 |\Phi|^2 + \lambda_h |H|^4 + \lambda_\phi |\Phi|^4 + \lambda_{h\phi} |H|^2 |\Phi|^2. \tag{3}$$

In this work, quadratic terms vanish at $M_{\rm Pl}$: $m_H^2(M_{\rm Pl}) = 0$ and $m_\Phi^2(M_{\rm Pl}) = 0$, and they are not even RG induced at lower scales (since we work with a mass-independent scheme of dimensional regularization) but only by spontaneous symmetry breaking, as will be discussed. We use the unitary gauge with $H = h/\sqrt{2}$ and $\Phi = \phi/\sqrt{2}$.

The one-loop CW effective potential of ϕ is

$$V(\phi) = \frac{1}{4}\lambda_\phi(M_{\rm Pl})\phi^4 + \frac{\phi^4}{64\pi^2}\left(10\lambda_\phi^2 + 48 g_X^4 - 8 y_N^4\right) \ln \frac{\phi^2}{M_{\rm Pl}^2} + \Delta V. \tag{4}$$

This can also be approximated in terms of the running coupling $\lambda_\phi(\phi)$ as

$$V(\phi) \simeq \frac{1}{4}(\lambda_\phi(\phi) + C)\phi^4 + \Delta V, \tag{5}$$

with the running

$$\lambda_\phi(\phi) \simeq \lambda_\phi(M_{\rm Pl}) + \beta_{\lambda_\phi} \ln \frac{\phi}{M_{\rm Pl}}. \tag{6}$$

We use the $\overline{\rm MS}$ scheme $C = 0$ so that $\lambda_\phi(M_{\rm Pl})$ directly measures the CMB amplitude $A_s \propto \lambda_\phi(M_{\rm Pl})$,[1] and ΔV will be determined soon. $M_{\rm Pl}$ is assumed to be the high-energy inflation scale, for simplicity. The form in Eq. (5) is convenient in matching the potential at the inflation scale. It is a good approximation to the correct Eq. (4) as the field-strength renormalizations, not explicitly appearing in Eq. (4) and denoted by $\cdots$ in

$$(4\pi)^2 \beta_{\lambda_\phi} = 20\lambda_\phi^2 + 96 g_X^4 - 16 y_N^4 + \cdots, \tag{7}$$

are small: $\mathcal{O}(\lambda_\phi g_X^2, \lambda_\phi y_N^2)$.

The potential is minimized at v_ϕ ($U(1)_X$ spontaneously broken) when

$$\lambda_\phi(v_\phi) = -\left(\frac{\beta_{\lambda_\phi}}{4} + C\right) = -\frac{1}{64\pi^2}\left(20\lambda_\phi^2 + 96 g_X^4 - 16 y_N^4\right)(v_\phi), \tag{8}$$

where $C = 0$. This requires $\lambda_\phi(v_\phi) \sim g_X^4, y_N^4 \ll g_X^2, y_N^2$, and such a hierarchical structure can be RG induced. Consequently, v_ϕ is exponentially suppressed compared to $M_{\rm Pl}$ by dimensional transmutation,

$$v_\phi \simeq M_{\rm Pl}\, e^{-\frac{1}{4}} \exp\left(-\frac{4\pi^2 \lambda_\phi(M_{\rm Pl})}{24 g_X^4(M_{\rm Pl}) - 4 y_N^4(M_{\rm Pl})}\right), \tag{9}$$

resolving the hierarchy problem; this is the CW mechanism. The symmetry breaking is subsequently transmitted to the SM Higgs potential through the portal mixing as

$$m_H^2(v_\phi) = \frac{1}{2}\lambda_{h\phi}(v_\phi) v_\phi^2. \tag{10}$$

[1] In Ref. [45], focusing on the CW mechanism for the EWSB, $C = -\frac{25}{12}\beta_{\lambda_\phi}(v_\phi)$ was chosen by the renormalization condition at low energy $\left.\frac{\partial^4 V}{\partial \phi^4}\right|_{\phi = v_\phi} = 6\lambda_\phi(v_\phi)$. C effectively only shifts the value of λ_ϕ.

Thus, the negative $\lambda_{h\phi}(v_\phi)$ is needed to break the electroweak symmetry too; such a negative value will also be RG induced—see Eq. (27). The electroweak vacuum expectation value $v_{\rm EW} \equiv \langle h \rangle$ is finally defined as

$$v_{\rm EW} = \sqrt{-\frac{m_H^2(v_{\rm EW})}{\lambda_h(v_{\rm EW})}}, \tag{11}$$

which is required to be 246 GeV.

The potential at the minimum $\phi = v_\phi$ is

$$V(\phi = v_\phi) = \frac{v_\phi^4}{4}(\lambda_\phi(v_\phi) + C) + \Delta V = -\frac{v_\phi^4}{16}\beta_{\lambda_\phi}(v_\phi) + \Delta V, \tag{12}$$

where the second equality used the minimization condition Eq. (8) and holds independently of C. The potential is non-zero and negative ($\beta_{\lambda_\phi}(v_\phi) > 0$) without ΔV. Thus, we set $\Delta V = +\frac{v_\phi^4}{16}\beta_{\lambda_\phi}(v_\phi)$ to make it zero and avoid unnecessary dark energy. This also necessarily affects the potential height at the inflation scale, but as discussed in the next section this is negligible at the inflation scale.

By this mechanism, even a strict flatland scenario starting with $\lambda_\phi(M_{\rm Pl}) = 0$ and $\lambda_{h\phi}(M_{\rm Pl}) = 0$ can successfully induce EWSB [45,46]. λ_ϕ has to be positive before it breaks $U(1)_X$ so that $\beta_{\lambda_\phi} < 0$ at high scales, but λ_ϕ must become negative to break $U(1)_X$, requiring β_{λ_ϕ} to flip its sign at some intermediate scale. This flip is achieved by the fine interplay of bosonic g_X and fermionic y_N contributions to the beta function,

$$(4\pi)^2\beta_{\lambda_\phi} \simeq 96g_X^4 - 16y_N^4, \tag{13}$$

with their respective running

$$(4\pi)^2\beta_{g_X} \simeq \left(12 - \frac{32}{3}x + \frac{41}{6}x^2\right)g_X^3, \qquad (4\pi)^2\beta_{y_N} \simeq 6y_N\left(y_N^2 - g_X^2\right). \tag{14}$$

As a result, for almost any $g_X(M_{\rm Pl})$ there exists a unique solution $y_N(M_{\rm Pl})$ for successful EWSB. The resulting collider phenomena depend on the value of $g_X(M_{\rm Pl})$. As shown in Ref. [45], the smaller $g_X(M_{\rm Pl})$ is, the smaller the corresponding $y_N(M_{\rm Pl})$ is. And, more relevantly, $M_X = 2g_X(v_\phi)v_\phi$ becomes larger and the Higgs mixing angle smaller (among many observables). But there is no definite range of such predictions since any value of $g_X(M_{\rm Pl})$ can induce EWSB. This is one crucial difference of our work.

In this paper, above all, we relax the condition $\lambda_\phi(M_{\rm Pl}) = 0$ in order to also explain inflation with the inflaton ϕ. As will be discussed, this brings definite ranges of low-energy predictions, leading to an intimate connection between high- and low-energy physics. Reference [47] considered such a scenario but with a different focus; Refs. [17,18] without EWSB. Later, we also relax $\lambda_{h\phi}(M_{\rm Pl}) = 0$, mainly to explore the dependence of our conclusion on this model parameter. A wider range of x is then allowed (see Ref. [46] for the allowed narrow range in a flatland), but only $x \sim 1$ will be considered to avoid too-large X charges; models with $x = 4/5$ and 2 can be obtained from the $SO(10)$ grand unified gauge group.

3. Inflation models for interpretation

In this section we introduce benchmark models of inflation that are simple enough to represent a large range of models and allow simple interpretations of low-energy results. The inflaton potential must also match the CW potential in Eq. (4) at low energy.[2]

[2]We assume here that the $B - L$ scalar ϕ is the main inflaton field and that the Higgs field does not play any roles during the inflation in order to connect the inflation and the low-energy collider observables

We start with a quartic chaotic inflation (as a warm-up and to show some basic features):

$$V(\phi) = \frac{\lambda_\phi(\mu=\phi)}{4}\phi^4 + \Delta V, \tag{15}$$

where $\lambda_\phi(\mu=\phi)$ is the running quartic coupling evaluated at $\mu=\phi$. This potential obviously matches the CW potential in Eq. (5) at low energy, again up to small field-strength renormalizations. We first show that the effect from ΔV introduced in Eq. (5) and determined in Eq. (12) is negligible. By rewriting the potential as $V+\Delta V = \frac{\lambda_\phi}{4}(1+\delta)M_{\rm Pl}^4$, the fractional correction

$$\delta \equiv \frac{\Delta V}{V(M_{\rm Pl})} = \frac{\beta_{\lambda_\phi}(v_\phi)}{4\lambda_\phi(\phi_I)}\left(\frac{v_\phi}{M_{\rm Pl}}\right)^4 \ll 1 \tag{16}$$

is negligible for only mildly suppressed $v_\phi \lesssim M_{\rm Pl}$ because $\beta_{\lambda_\phi} \sim g_X^4 \sim y_N^4$ and $\lambda_\phi(M_{\rm Pl}) = 10^{-4,\,-8}$, $g_X = 10^{-3} \sim 10^{-1}$, are relevant in this work (see the next section).

This simple model shows that the CMB amplitude directly measures the potential height at the inflation scale,

$$A_s = \frac{1}{24\pi^2}\frac{V}{M_{\rm Pl}^4}\frac{1}{\epsilon} \simeq 5.76\times 10^5 \frac{\lambda_\phi(M_{\rm Pl})}{\pi^2}, \tag{17}$$

so that very small $\lambda \simeq 4\times 10^{-14}$ is needed to explain the observed Planck 2018 data [1,2],

$$A_s = 2.101^{+0.031}_{-0.034}\times 10^{-9} \qquad (68\%\ \text{confidence level (CL)}), \tag{18}$$

where the CMB observables are evaluated at the pivot scale $k_* = 0.05\,{\rm Mpc}^{-1}$ with $N=60$. But this minimal model predicts too large a tensor-to-scalar ratio r,

$$r = 16\varepsilon \simeq \frac{16}{N}, \qquad n_s = 1-6\varepsilon+2\eta \simeq 1-\frac{3}{N}, \tag{19}$$

compared to the Planck data:

$$r < 0.056 \quad (95\%\text{CL}),$$
$$n_s = 0.9665 \pm 0.0038,\ \frac{dn_s}{d\ln k} = 0.013\pm 0.024\ (68\%\ \text{CL}). \tag{20}$$

3.1 *Inflation with non-minimal coupling*

Our main benchmark model is the quartic potential with a non-minimal coupling $\xi\phi^2 R/M_{\rm Pl}^2$ (with dimensionless $\xi > 0$) between inflaton and gravity [10,19–28]. This model is known to realize successful inflation, and the single new parameter ξ allows easy interpretation of our results.

This model works as ξ effectively suppresses the quartic potential at the inflation scale,

$$V_{\rm E} = \frac{\lambda_\phi}{4}\frac{\phi^4}{\Omega^4}, \qquad \Omega^2 = 1+\xi\left(\frac{\phi}{M_{\rm Pl}}\right)^2 > 1, \tag{21}$$

where the subscript E refers to the Einstein frame; a canonical normalization of ϕ brings additional modifications but this is the basic structure. Thus, ξ becomes effective for large-field inflation $\phi \gtrsim M_{\rm Pl}/\sqrt{\xi}$. In this limit, similarly to the conventional Higgs inflation case, the CMB observables are

$$r \simeq \frac{12}{N^2}, \qquad n_s \simeq 1-\frac{2}{N}, \qquad A_s \simeq \frac{\lambda_\phi(M_{\rm Pl})N^2}{72\pi^2\xi^2}. \tag{22}$$

such as the Z' mass. (See also Refs. [51–53] and references therein for a singlet scalar extension.) The field (parameter) space where the Higgs field plays the role of dominant inflaton is less attractive because the inflation prediction is not necessarily related to the symmetry-breaking sector. We will also discuss such a field (parameter) space in a future investigation.

Not only can r and n_s be consistent with the Planck data, but we also obtain the following relation between $\lambda_\phi(M_{\rm Pl})$ and ξ by the CMB amplitude $A_s \simeq 2.1 \times 10^{-9}$ in Eq. (18):

$$\frac{\lambda_\phi(M_{\rm Pl})}{\xi^2} \simeq 4.1 \times 10^{-10} \left(\frac{60}{N}\right)^2 . \tag{23}$$

The larger $\lambda_\phi(M_{\rm Pl})$, the larger the field value at the inflation scale, and hence larger suppression by ξ is needed.

How large or small values of ξ are natural, or most preferred? Since we do not specify a fundamental theory that might be able to calculate the value of ξ, it is naively reasonable to consider $\xi \sim \mathcal{O}(1)$ as a natural value. If we restrict $\xi \lesssim 100$, for example, the required size of $\lambda_\phi(M_{\rm Pl}) \lesssim 10^{-6}$ can be significantly larger (hence, more natural or likely) than the naive translation 10^{-14} mentioned in the introduction, albeit still too small to be perfectly natural. On the other hand, there exists a lower bound on ξ. In the limit of $\xi \to 0$, the theory asymptotes to a pure quartic potential, which is inconsistent with observations as discussed in Eq. (19). We have numerically checked that $\xi \gtrsim 0.01$ in order to be consistent with CMB observations; the above large-ϕ approximation starts to break down for $\xi \lesssim 0.1$ (or $\lambda_\phi(M_{\rm Pl}) \lesssim 10^{-11}$). It is also possible for $\lambda_\phi \sim \mathcal{O}(1)$ to be natural with much larger $\xi \sim 10^5$, but usually too-strong interactions can produce various unexpected corrections too. Thus, we will regard $0.01 \lesssim \xi \lesssim 100$ (or $10^{-12} \lesssim \lambda_\phi(M_{\rm Pl}) \lesssim 10^{-6}$) as the most desired (natural and comfortable) parameter space of inflation. Later, we will see that this is exactly the parameter space that is preferred by the low-energy constraints.

Lastly, we comment on the reheating after inflation. In usual $U(1)_X$ models, the transfer of energy from inflatons to radiation can occur through perturbative decays, $\phi \to Z'Z'$ ($\nu_R\nu_R$), or non-perturbative particle production caused by the oscillation of ϕ. For $\lambda_\phi(M_{\rm Pl}) \gtrsim 10^{-3}$ (or $\xi \gtrsim 10^3$), the qualitative behaviors of the preheating are expected to resemble those of Higgs inflation because ϕ couples to Z' (ν_R) in a similar way to H coupling to W, Z (ν_R). Thus, the reheating can occur instantaneously and the reheat temperature $T_{\rm R}$ can be high, $\mathcal{O}(\rho_{\rm inf}^{1/4}) = \mathcal{O}(\lambda_\phi^{1/2} M_{\rm Pl}/\xi^{1/2})$ [54–57]. On the other hand, for $\lambda_\phi(M_{\rm Pl}) \ll 10^{-3}$ (or $\xi \ll 10^3$), the $U(1)_X$ gauge coupling g_X can become much smaller than the SM gauge couplings. Such a small coupling prevents rapid perturbative decays of Z' into SM fermions as well as reducing the efficiency of parametric resonances. But some conventional studies [58,59] still predict a sufficiently large reheat temperature,[3] and Ref. [60] shows that the existence of higher-dimensional operators such as $(\partial\phi)^4/(M_{\rm Pl}/\sqrt{\xi})^2$ can significantly alter the preheating dynamics. Thus, (p)reheating with non-minimal couplings is model dependent, and more dedicated estimates are beyond the scope of this paper.

3.2 *α-attractor models*

The α-attractor model [30–33] is another benchmark model. Its inflation predictions are universal as long as the inflaton potential is smooth around the pole $\phi = \sqrt{6}M_{\rm Pl}$ of the kinetic

[3] For example, Ref. [58] shows that for $\xi \sim 1 (\lambda_\phi \sim 10^{-8})$ and $g_X \sim 0.01$, the ratio of energy densities between Z' and ϕ is roughly given by $\sim 10^{-4}(2.7)^j/\sqrt{j}$, where j is the number of zero crossings of ϕ. This becomes $\mathcal{O}(1)$ for $j \sim 10$, which corresponds to large radiation energy $\rho_R \sim \rho_\phi \sim \lambda_\phi M_{\rm Pl}^4/(6\pi^2\xi^2 j^2) \sim (10^{-3} M_{\rm Pl})^4$.

term. The predictions are

$$r \simeq \frac{12\alpha}{N^2}, \qquad n_s \simeq 1 - \frac{9\alpha}{2N^2} - \frac{2}{N}, \qquad A_s \simeq \frac{V_0 N^2}{18\pi^2 \alpha M_{\rm Pl}^4}, \tag{24}$$

where V_0 is the height of the inflaton potential at $\phi = \sqrt{6}M_{\rm Pl}$. In the case of the quartic potential in Eq. (15), we have

$$A_s = \frac{\lambda_\phi(M_{\rm Pl})N^2}{2\pi^2\alpha}, \qquad \therefore \ \frac{\lambda_\phi(M_{\rm Pl})}{\alpha} \simeq 1.2 \times 10^{-11} \times \left(\frac{60}{N}\right)^2, \tag{25}$$

where the running of $\lambda_\phi(\phi)$ is neglected. Thus, as in the non-minimal-coupling case, α is determined as a function of $\lambda_\phi(M_{\rm Pl})$. From the n_s data in Eq. (20) $\alpha \lesssim 10$ at the $2\,\sigma$ level, and hence $\lambda_\phi(M_{\rm Pl}) \lesssim 10^{-10}$. Thus, the allowed values of $\lambda_\phi(M_{\rm Pl})$ are somewhat smaller than those of the non-minimal-coupling case.

As for the preheating, it was found that the effective mass of ϕ becomes tachyonic after inflation [61], so that careful analysis is often necessary to estimate particle production and the resulting reheat temperature; see, for example, Refs. [62–64] and references therein.

4. Probing the small CMB amplitude by low-energy physics

4.1 *Main reason for low-energy probes of high-energy physics*

The most crucial reason for the existence of this intriguing connection is that for given $\lambda_\phi(M_{\rm Pl}) \neq 0$ there exists a *maximum* M_X (the strongest low-energy constraints among many observables) consistent with successful EWSB. Consequently, a definite range of $\lambda_\phi(M_{\rm Pl})$, which is directly related to the CMB observables at the inflation scale, can be probed with low-energy constraints on M_X.

The explanation begins with the existence of the minimum $g_X(M_{\rm Pl})$ for a given $\lambda_\phi(M_{\rm Pl}) \neq 0$. A smaller $g_X(M_{\rm Pl})$ generally induces smaller (negative) RG corrections to $\lambda_{h\phi}$ ($\lambda_{h\phi}(M_{\rm Pl}) = 0$) so that a larger v_ϕ is needed to produce a correct $v_{\rm EW} = 246\,{\rm GeV}$ from Eqs. (10) and (11),

$$v_{\rm EW} \sim \sqrt{-\frac{\lambda_{h\phi}(v_\phi)}{\lambda_h(v_{EW})}}\, v_\phi \lesssim v_\phi, \tag{26}$$

where the last inequality is due to $|\lambda_{h\phi}| \ll \lambda_h \sim 0.1$. A larger v_ϕ needs larger $24g_X^4(M_{\rm Pl}) - 4y_N^4(M_{\rm Pl})$ in the dimensional transmutation of v_ϕ in Eq. (9). In any case, too small a $g_X(M_{\rm Pl})$ would require too large a $v_\phi \gtrsim M_{\rm Pl}$ to be realized in this model, hence the existence of the minimum $g_X(M_{\rm Pl})$.[4]The existence is proved numerically in Fig. 1, where the minimum $g_X(M_{\rm Pl})$ is marked with a square dot for each $\lambda_\phi(M_{\rm Pl})$ and for each $x = 4/5$ and 2. The values of the minimum $g_X(M_{\rm Pl})$ depend weakly on x, as the exponential dimensional transmutation of v_ϕ does not strongly depend on x.

The minimum $g_X(M_{\rm Pl})$ leads to the maximum M_X for a given $\lambda_\phi(M_{\rm Pl})$, because the smaller $g_X(M_{\rm Pl})$ corresponds to the larger v_ϕ, as discussed (see also Ref. [45]). Since v_ϕ depends exponentially on g_X, the resulting $M_X = 2g_X(v_\phi)v_\phi$ is larger (Higgs mixing smaller). Thus, the minimum $g_X(M_{\rm Pl})$ is translated to the maximum M_X, as also shown numerically in Fig. 1. Moreover, a larger $v_\phi \gg v_{\rm EW}$ leads to smaller Higgs mixing corrections to Higgs couplings. The values of the maximum M_X depend on $\lambda_\phi(M_{\rm Pl})$ and x. First, a larger $\lambda_\phi(M_{\rm Pl})$ typically needs a larger $g_X(M_{\rm Pl})$ to RG-drive λ_ϕ negative (for symmetry breaking). This also necessarily induces a larger portal

[4]Note that Eq. (9) depends directly on $\lambda_\phi(M_{\rm Pl})$ so that this argument does not directly apply to flatland scenarios with $\lambda_\phi(M_{\rm Pl}) = 0$.

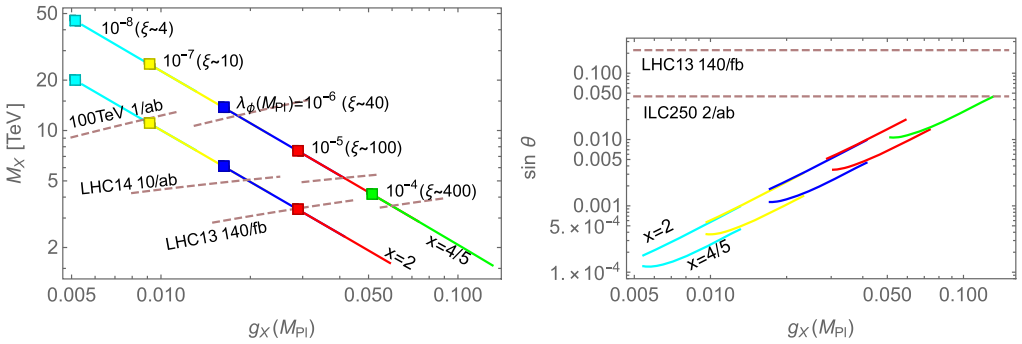

Fig. 1. M_X (left) and Higgs mixing $\sin\theta$ (right) predicted by solutions for correct EWSB, parameterized by $\lambda_\phi(M_{\rm Pl})$ and $g_X(M_{\rm Pl})$ for two different choices of $x = 4/5$ and 2. For each λ_ϕ shown as a different color (also marked with the ξ value for the correct CMB amplitude), the minimum g_X and corresponding maximum M_X (and minimum $\sin\theta$) are marked as square dots; large-g_X regions of different colors overlap. Recast collider bounds from Z' searches and precision Higgs coupling measurements are shown as dashed lines. $\lambda_{h\phi}(M_{\rm Pl}) = 0$.

mixing $|\lambda_{h\phi}(v_\phi)|$, so a smaller v_ϕ yields a correct EW scale via Eq. (26). Thus, larger $\lambda_\phi(M_{\rm Pl})$ predicts smaller maximum M_X (and larger Higgs mixing). Second, the x dependence arises mainly from the running of $\lambda_{h\phi}$,

$$(4\pi)^2\beta_{\lambda_{h\phi}} \simeq 12 g_X^4 x^2. \tag{27}$$

Roughly speaking, the larger x, the larger $|\lambda_{h\phi}(v_\phi)|$ at v_ϕ, so that a smaller v_ϕ can induce a correct $v_{\rm EW}$, resulting in smaller maximum M_X. These behaviors are shown in Fig. 1.

This is the main feature of the models where inflation and the CW mechanism of EWSB are induced by a common particle.

4.2 *Results: Collider probes of inflation*

It turns out that the constraints on M_X (from Z' collider searches) provide the strongest probe. The current bound on the mass of Z' having the same interactions as the SM Z is 5.1 TeV from LHC 13 140 fb^{-1} [65,66]. It is interpreted as the current bound on M_X with LHC 13 140 fb^{-1}, and recast for high-luminosity LHC 14 with 10 ab^{-1} and future 100 TeV pp colliders with 1 ab^{-1}. The results are shown in Fig. 1 as dashed lines for each x. How we recast the M_X bounds and obtain bounds on the parameter space as shown in the figures is described in Appendix A.

Z' searches provide a meaningful probe of the inflation sector. For the model with $x = 2$ shown in Fig. 1, a 100 TeV collider can probe $\lambda_\phi(M_{\rm Pl}) \gtrsim 10^{-7}$ ($\xi \gtrsim 10$) *definitely*. This means first that larger values of λ_ϕ and ξ cannot induce correct EWSB while being consistent with CMB and Z' searches. But this does not mean that the whole parameter space with a smaller $\lambda_\phi(M_{\rm Pl})$ can explain all CMB, EWSB, and Z'; rather, there exists some working parameter space, which usually yields small g_X and heavy M_X. In this sense, we will say that a 100 TeV collider with 1 ab^{-1} has a (definite) reach down to $\lambda_\phi(M_{\rm Pl}) \simeq 10^{-7}$ and $\xi \sim 10$ for $x = 2$; the less natural size of $\xi \gtrsim 10$ will be more strongly constrained by 100 TeV collider searches.

Figure 2 shows such *definite* bounds (using the maximum M_X for the given parameters) in a more general parameter space of x–$\lambda_\phi(M_{\rm Pl})$. The shaded regions are excluded by the recast bounds on M_X; for given $\lambda_\phi(M_{\rm Pl})$ and x within these regions, the maximum M_X is lighter than the recast bounds. Note that both recast bounds and maximum M_X (dotted contours) vary with x and $\lambda_\phi(M_{\rm Pl})$ as well as with the collider specification. Also overlapped are the contours

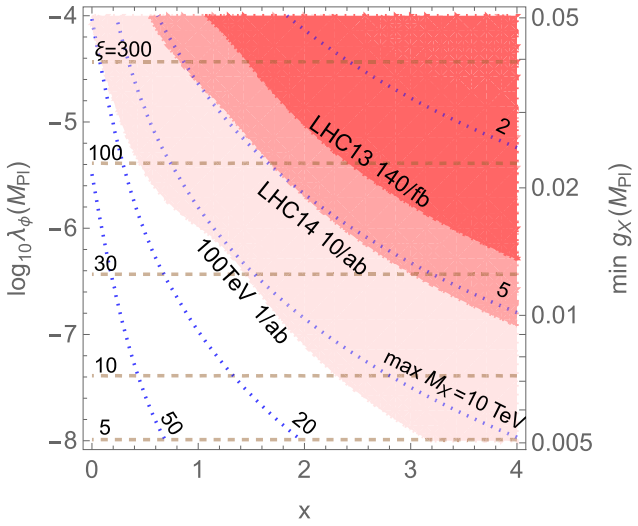

Fig. 2. Collider constraints on the parameter space of inflation with non-minimal coupling ξ and the Coleman–Weinberg Higgs mechanism. On each point on the plane of $\lambda_\phi(M_{\rm Pl})$ and x, the minimum $g_X(M_{\rm Pl})$ for correct EWSB and the corresponding maximum M_X (blue dashed) are used to obtain collider constraints from Z' searches. The red shaded regions are definite bounds, within which no parameter space can induce correct EWSB while being consistent with Z' searches. From darkest to lightest shaded regions are the bounds from current LHC 13 140 fb^{-1}, high-luminosity LHC 14 10 ab^{-1} projection, and future 100 TeV pp collider 1 ab^{-1} projection. Also shown as horizontal dashed lines are the required value of ξ for the correct CMB amplitude as in Eq. (23); the most natural range of $\xi \lesssim \mathcal{O}(1$–$100)$ is preferred. $\lambda_{h\phi}(M_{\rm Pl}) = 0$.

of ξ (horizontal dashed) for the correct CMB amplitude. In general, ξ can be more strongly constrained for larger x, as discussed; a pure $B-L$ model with $x=0$ is much harder to probe. Due to this x-dependence, it is not appropriate to find a strict upper bound on ξ. But, we conclude that a large part of $\lambda_\phi \gtrsim \mathcal{O}(10^{-4}$–$10^{-6})$ or $\xi \gtrsim \mathcal{O}(10$–$100)$ can be probed with the current LHC 13 35 fb^{-1} and LHC 13 10 ab^{-1}; and $\xi \gtrsim \mathcal{O}(1$–$10)$ with a 100 TeV pp collider at 1 ab^{-1}. As discussed in Section 3, the allowed range of ξ may be considered most natural. Likewise, in the α-attractor model, using Eqs. (23) and (25), we conclude that a large part of $\alpha \gtrsim 10^6$–10^5 and 10^5–10^3 can be probed, respectively.

Lastly, Higgs-related physics gives weaker bounds but can still be relevant. Higgs physics is modified by small portal mixing $\lambda_{h\phi}(v_\phi) = 10^{-9} \sim 10^{-4}$, for $g_X = 0.005$–0.1 respectively. The resulting Higgs mixing angle is

$$\sin\theta \simeq \lambda_{h\phi}(v_\phi) v_\phi v_{EW}/m_h^2 \sim \sqrt{\lambda_{h\phi}(v_\phi)/2\lambda_h} = 10^{-4}\sim 10^{-1}, \tag{28}$$

as also shown in the right panel of Fig. 1. But these are too small to be probed with the current LHC precision $\sin\theta \lesssim 0.26$ with 140 fb^{-1} [67–70], as well as with the expected precision $\sin\theta \lesssim 0.045$ from ILC 250 S2 stage with 2 ab^{-1} [71,72]. In addition, ϕ is expected to be light, $M_\phi \simeq \sqrt{\frac{6}{11}\lambda_\phi(v_\phi)} v_\phi = \mathcal{O}(0.1$–$10)$ GeV for most of the parameter space, but the $h \to \phi\phi$ decay rate is still too small at $\Gamma(h \to \phi\phi) \simeq \frac{\lambda_{h\phi}(v_\phi)^2 v_{\rm EW}^2}{32\pi m_h} \sqrt{1 - \frac{4m_\phi^2}{m_h^2}} \lesssim 10^{-3}$ MeV (or its branching ratio $\lesssim 10^{-3}$) to be probed even at ILC 250, whose expected precision on the invisible decay branching ratio is $\sim$0.003 [71,72]. LHCb, BaBar, and Belle are sensitive to GeV-scale dark photons with interaction strength $\epsilon \gtrsim 10^{-3}$–10^{-4} [73], but the ϕ–lepton interaction yields too small

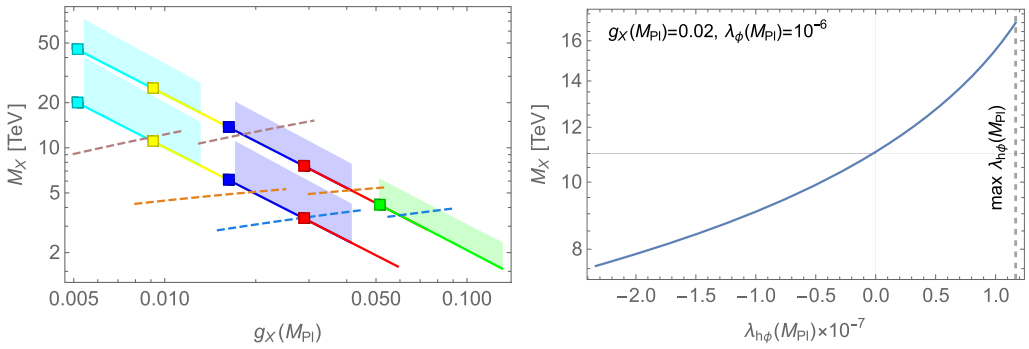

Fig. 3. Left: As Fig. 1, but showing variations of low-energy predictions with $\lambda_{h\phi}(M_{\rm Pl}) > 0$ (shaded regions). The shaded regions still have definite ranges determined by the maximum positive $\lambda_{h\phi}(M_{\rm Pl})$ in Eq. (29) that can induce correct EWSB, which yields a somewhat heavier M_X for given $g_X(M_{\rm Pl})$. Right: An example M_X prediction as a function of $\lambda_{h\phi}(M_{\rm Pl})$ for fixed $g_X(M_{\rm Pl}) = 0.02$ and $\lambda_\phi(M_{\rm Pl}) = 10^{-6}$. The maximum $\lambda_{h\phi}(M_{\rm Pl})$ consistent with EWSB is marked as a vertical dashed line. See text for more discussion.

an $\epsilon = \frac{y_e}{e}\sin\theta \simeq 9.2\times10^{-6}\sin\theta \ll 10^{-3}$ in this scenario. Nevertheless, as discussed, Higgs-related physics can be important for proper reheating.

4.3 *Variation with non-zero portal mixing*

We now assess the variation with $\lambda_{h\phi}(M_{\rm Pl}) \neq 0$. It cannot be arbitrarily large positive for given $g_X(M_{\rm Pl})$. Since $\lambda_{h\phi}(v_\phi) < 0$ has to be negative to induce EWSB, its RG running should be large enough,

$$\Delta\lambda_{h\phi} \simeq \beta_{\lambda_{h\phi}} \cdot \log\left(\frac{v_\phi}{M_{\rm Pl}}\right) \simeq \frac{12 g_X^4 x^2}{(4\pi)^2} \cdot \mathcal{O}(10) \gtrsim \lambda_{h\phi}(M_{\rm Pl}). \tag{29}$$

Thus, for given $g_X(M_{\rm Pl})$ (and $\lambda_\phi(M_{\rm Pl})$), there exists a maximum $\lambda_{h\phi}(M_{\rm Pl})$ inducing correct EWSB. Importantly, this still yields a maximum M_X for the given parameters because larger positive $\lambda_{h\phi}(M_{\rm Pl})$ yields a smaller $|\lambda_{h\phi}(v_\phi)|$, hence requiring a larger v_ϕ, yielding heavier M_X. The maximum M_X will be larger for $\lambda_{h\phi}(M_{\rm Pl}) > 0$, but the maximum still exists. In the other limit of negative $\lambda_{h\phi}(M_{\rm Pl}) < 0$, the maximum M_X is smaller, so is more strongly constrained. These are numerically shown proved in Fig. 3; the modified maximum M_X is shown in the left panel as shaded regions, and the maximum M_X as a function of $\lambda_{h\phi}(M_{\rm Pl})$ is shown in the right panel where the maximum positive $\lambda_{h\phi}(M_{\rm Pl})$ for EWSB is marked as a vertical line. The new maximum M_X is larger by a factor of 1.5–2.0.

In Fig. 4 we show definite bounds with maximum positive $\lambda_{h\phi}(M_{\rm Pl})$ (worst constraints) as well as with negative $\lambda_{h\phi}(M_{\rm Pl})$ with twice the magnitude (stronger constraints). Again, the shaded regions are definite bounds, within which no parameter space can be consistent with all CMB, EWSB, and collider searches. For the former case, current LHC 13 140 fb^{-1} can still probe a large part of $\xi \gtrsim \mathcal{O}(100)$, and future high-luminosity LHC 14 10 ab^{-1} and 100 TeV $p\bar{p}$ with 1 ab^{-1} can probe a large part of $\xi \gtrsim 100$–10. But this is for the maximum $\lambda_{h\phi}(M_{\rm Pl})$ yielding the worst constraints; $\lambda_{h\phi}$ would more likely take a smaller or negative value. In such a case (right panel), the constraints/prospects are stronger, and the majority of $\xi \gtrsim 1$–10 can be probed with future 100 TeV 1 ab^{-1}, and current LHC 13 140 fb^{-1} can already probe a large part of $\xi \gtrsim \mathcal{O}(100)$. In any case, smaller ξ will be preferred by collider experiments.

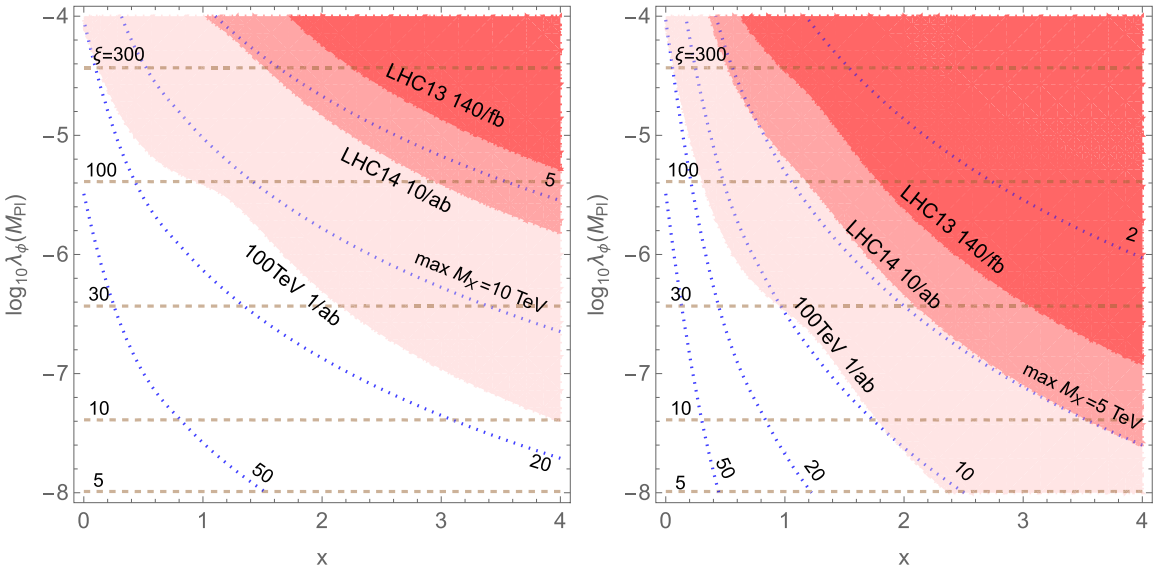

Fig. 4. As Fig. 2, but now with $\lambda_{h\phi}(M_{\rm Pl}) \neq 0$: maximum positive $\lambda_{h\phi}(M_{\rm Pl}) > 0$ for EWSB as in Eq. (29) and Fig. 3 yielding heavier maximum M_X (left panel), and negative $\lambda_{h\phi}(M_{\rm Pl}) < 0$ with twice the magnitude yielding lighter maximum M_X (right panel).

5. Summary

We have shown that the existence of the upper range of M_X allows the parameter space for the small CMB amplitude to be probed by collider experiments. In the inflation model with non-minimal coupling ξ, the absence of collider signals of Z' at LHC 13 and 100 TeV pp will prefer a smaller and more natural size of $\xi \lesssim 1$–100 with $\lambda_\phi(M_{\rm Pl}) \lesssim 10^{-4}$–$10^{-8}$ even though ξ could equally well take a much larger value to explain the CMB amplitude. For example, the models with $\lambda_\phi(M_{\rm Pl}) \sim \mathcal{O}(1)$ and $\xi \sim 10^5 \gg 1$ will be strongly constrained. A similar conclusion for an α-attractor model is obtained, albeit more weakly.

This probe was possible in models where an inflaton ϕ also induces EWSB via perturbative quantum corrections (the CW mechanism). It was the restrictions on the ϕ potential from well-measured high-energy inflation and low-energy electroweak physics that led to intimate correlations between low-energy M_X (collider observables) and high-energy $\lambda_\phi(M_{\rm Pl})$ (the CMB amplitude $A_s \propto \lambda_\phi(M_{\rm Pl})$). More crucially, there exists an upper range of M_X prediction for each value of $\lambda_\phi(M_{\rm Pl})$, so that definite collider constraints on $\lambda_\phi(M_{\rm Pl})$ could be derived.

This work not only proves the interesting possibility of probing the inflation sector with low-energy experiments, but may also relate the absence of new physics signals to the physics at a disparate energy scale. Although this connection may not be general and it does not explain why such a small CMB amplitude is realized in our universe, the fact that some particular high-energy realization has consequences in low-energy physics is intriguing enough, and is worth studying in a wider range of models and contexts.

Acknowledgments

We are supported by Grant Korea NRF-2019R1C1C1010050 and 2019R1A6A1A10073437, and S. J. also by a POSCO Science Fellowship.

Funding

Open Access funding: SCOAP[3].

Appendix A. Methods

In this appendix we elaborate on our method of recasting collider constraints.

We recast narrow-resonance searches by following the Collider Reach method [74]. It is based on the narrow-resonance invariant mass (in our case) being so powerful and simple a discriminant that other kinematical and distribution observables are less important. The search becomes essentially characterized by a single energy scale M_X (for given other collider specifications). Moreover, if the signal and background are initiated by the same partons, then the already optimized search performance will remain similar for a range of collision energies and resonance masses. The mass reach can then be simply rescaled by cross-section ratios or the number of events (before cuts). In other words, the new reach on M_X is where the same number of events (before cuts) are produced.

This method is known to work well for narrow-resonance searches. If it did not, this would have to be explained e.g. by some newly understood/added components in the analysis. Indeed, it has been used in the theoretical community for quick estimations of collider prospects; see, e.g., Refs. [75–77]. More details, caveats, and example calculations are provided in Ref. [74].

Our M_X reaches in Figs. 1, 2, 3, and 4 are obtained in this way. They are where the same number of dilepton events are produced as the latest LHC reaches (5.1 TeV sequential Z' [65,66]). This method is reasonable as the signal and dominant background processes are all $q\bar{q}$-initiated, and the resonances are narrow. No Monte Carlo is used, and more dedicated estimates are beyond the scope of this paper.

The bounds on the model parameter space need more elaboration. M_X and its couplings to fermions are not input parameters but rather low-energy parameters determined by the high-energy input parameters $g_X(M_{\rm Pl})$ and $\lambda_\phi(M_{\rm Pl})$. Once we obtain them in each parameter space (as we describe below), we calculate branching ratios to dileptons, relative fractions of $u\bar{u}$ and $d\bar{d}$ initial partons (MSTW2008NLO [78]), hence cross-section ratios to find new reaches. All these are taken into account, and they show up as the complicated shapes of the constraints.

To obtain low-energy parameters for given $g_X(M_{\rm Pl})$ and $\lambda_\phi(M_{\rm Pl})$ inputs, we numerically solve the renormalization group equations and find $y_N(M_{\rm Pl})$ and v_ϕ producing correct EWSB from Eqs. 8, (10), and (11). Then, we can calculate $M_X = 2g_X(v_\phi)v_\phi$, couplings to fermions, and finally the number of dilepton events. These are used to recast M_X reaches and obtain collider bounds on the parameter space. In Figs. 3 and 4 we also vary the non-zero $\lambda_{h\phi}(M_{\rm Pl})$ input, allowing a wider range of results.

After all this, it turns out that the successful parameter space restricts the (upper) range of M_X so that we can make some definite collider prospects. Such relations are not simply captured by a few equations, but discussed in various levels of detail throughout Section 4 (in particular, Section 4.1). This is the main point of this paper.

References

[1] N. Aghanim et al. Astron. Astrophys. **641**, A6 (2020).
[2] Y. Akrami et al. Astron. Astrophys. **641**, A10 (2020).
[3] M. Tegmark and M. J. Rees, Astrophys. J. **499**, 526 (1998).
[4] A. Vilenkin, Phys. Rev. Lett. **74**, 846 (1995).

[5] D. Buttazzo, G. Degrassi, P. P. Giardino, G. F. Giudice, F. Sala, A. Salvio, and A. Strumia, J. High Energy Phys. **12**, 089 (2013).
[6] J. Elias-Miro, J. R. Espinosa, G. F. Giudice, G. Isidori, A. Riotto, and A. Strumia, Phys. Lett. B **709**, 222 (2012).
[7] G. Degrassi, S. Di Vita, J. Elias-Miro, J. R. Espinosa, G. F. Giudice, G. Isidori, and A. Strumia, J. High Energy Phys. **08**, 098 (2012).
[8] A. V. Bednyakov, B. A. Kniehl, A. F. Pikelner, and O. L. Veretin, Phys. Rev. Lett. **115**, 201802 (2015).
[9] Y. Hamada, H. Kawai, and K.-Y. Oda, Phys. Rev. D **87**, 053009 (2013) 89, 059901 (2014) [erratum].
[10] F. L. Bezrukov and M. Shaposhnikov, Phys. Lett. B **659**, 703 (2008).
[11] F. Bezrukov and M. Shaposhnikov, J. High Energy Phys. **07**, 089 (2009).
[12] F. Bezrukov, A. Magnin, M. Shaposhnikov, and S. Sibiryakov, J. High Energy Phys. **01**, 016 (2011).
[13] A. Salvio, Phys. Lett. B **727**, 234 (2013).
[14] Y. Hamada, H. Kawai, and K. Kawana, Prog. Theor. Exp. Phys. **2015**, 091B01 (2015).
[15] G. Ballesteros and C. Tamarit, J. High Energy Phys. **02**, 153 (2016).
[16] S.-M. Choi and H. M. Lee, Eur. Phys. J. C **76**, 303 (2016).
[17] N. Okada and D. Raut, Phys. Rev. D **95**, 035035 (2017).
[18] N. Okada, S. Okada, and D. Raut, Phys. Rev. D **95**, 055030 (2017).
[19] Y. Hamada, H. Kawai, K.-Y. Oda, and S. C. Park, Phys. Rev. D **91**, 053008 (2015).
[20] A. O. Barvinsky, A. Yu. Kamenshchik, and A. A. Starobinsky, J. Cosmol. Astropart. Phys. **11**, 021 (2008).
[21] A. De Simone, M. P. Hertzberg, and F. Wilczek, Phys. Lett. B **678**, 1 (2009).
[22] K. Allison, J. High Energy Phys. **02**, 040 (2014).
[23] Y. Hamada, H. Kawai, and K.-Y. Oda, Prog. Theor. Exp. Phys. **2014**, 023B02 (2014).
[24] Y. Hamada, H. Kawai, K.-Y. Oda, and S. C. Park, Phys. Rev. Lett. **112**, 241301 (2014).
[25] F. Bezrukov and M. Shaposhnikov, Phys. Lett. B **734**, 249 (2014).
[26] Y. Hamada, H. Kawai, and K.-Y. Oda, J. High Energy Phys. **07**, 026 (2014).
[27] Y. Hamada, H. Kawai, Y. Nakanishi, and K.-Y. Oda, Nucl. Phys. B **953**, 114946 (2020).
[28] Y. Hamada, H. Kawai, K. Kawana, K.-Y. Oda, and K. Yagyu, arXiv:2102.04617 [hep-ph] [Search inSPIRE].
[29] S. C. Park and S. Yamaguchi, J. Cosmol. Astropart. Phys. **08**, 009 (2008).
[30] S. Ferrara, R. Kallosh, A. Linde, and M. Porrati, Phys. Rev. D **88**, 085038 (2013).
[31] R. Kallosh, A. Linde, and D. Roest, J. High Energy Phys. **11**, 198 (2013).
[32] M. Galante, R. Kallosh, A. Linde, and D. Roest, Phys. Rev. Lett. **114**, 141302 (2015).
[33] R. Kallosh and A. Linde, J. Cosmol. Astropart. Phys. **07**, 002 (2013).
[34] C. D. Froggatt and H. B. Nielsen, Phys. Lett. B **368**, 96 (1996).
[35] C. D. Froggatt, H. B. Nielsen, and Y. Takanishi, Phys. Rev. D **64**, 113014 (2001).
[36] H. B. Nielsen, Bled Workshops Phys. **13**, 94 (2012).
[37] H. Kawai and T. Okada, Int. J. Mod. Phys. A **26**, 3107 (2011).
[38] H. Kawai and T. Okada, Prog. Theor. Phys. **127**, 689 (2012).
[39] H. Kawai, Int. J. Mod. Phys. A **28**, 1340001 (2013).
[40] Y. Hamada, H. Kawai, and K. Kawana, Int. J. Mod. Phys. A **29**, 1450099 (2014).
[41] Y. Hamada, H. Kawai, and K. Kawana, Prog. Theor. Exp. Phys. **2015**, 033B06 (2015).
[42] Y. Hamada, H. Kawai, and K. Kawana, Prog. Theor. Exp. Phys. **2015**, 123B03 (2015).
[43] Y. Hamada, H. Kawai, and K.-Y. Oda, Phys. Rev. D **92**, 045009 (2015).
[44] K. Kannike, N. Koivunen, and M. Raidal, arXiv:2010.09718 [hep-ph] [Search inSPIRE].
[45] E. J. Chun, S. Jung, and H. M. Lee, Phys. Lett. B **725**, 158 (2013) **730**, 357 (2014) [erratum].
[46] M. Hashimoto, S. Iso, and Y. Orikasa, Phys. Rev. D **89**, 016019 (2014).
[47] K. Kawana, Prog. Theor. Exp. Phys. **2015**, 073B04 (2015).
[48] S. Oda, N. Okada, D. Raut, and D.-S. Takahashi, Phys. Rev. D **97**, 055001 (2018).
[49] N. Okada and D. Raut, Phys. Rev. D **103**, 055022 (2021).
[50] S. Kawai, N. Okada, and S. Okada, Phys. Rev. D **103**, 035026 (2021).
[51] O. Lebedev and H. M. Lee, Eur. Phys. J. C **71**, 1821 (2011).
[52] R. N. Lerner and J. McDonald, Phys. Rev. D **80**, 123507 (2009).
[53] N. Okada and Q. Shafi, Phys. Rev. D **84**, 043533 (2011).

[54] M. P. DeCross, D. I. Kaiser, A. Prabhu, C. Prescod-Weinstein, and E. I. Sfakianakis, Phys. Rev. D **97**, 023526 (2018).
[55] M. P. DeCross, D. I. Kaiser, A. Prabhu, C. Prescod-Weinstein, and E. I. Sfakianakis, Phys. Rev. D **97**, 023527 (2018).
[56] M. P. DeCross, D. I. Kaiser, A. Prabhu, and C. and E. I. Sfakianakis, Phys. Rev. D **97**, 023528 (2018).
[57] E. I. Sfakianakis and J. van de Vis, Phys. Rev. D **99**, 083519 (2019).
[58] J. Garcia-Bellido, D. G. Figueroa, and J. Rubio, Phys. Rev. D **79**, 063531 (2009).
[59] F. Bezrukov, D. Gorbunov, and M. Shaposhnikov, J. Cosmol. Astropart. Phys. **06**, 029 (2009).
[60] Y. Hamada, K. Kawana, and A. Scherlis, J. Cosmol. Astropart. Phys. **03**, 062 (2021).
[61] Y. Ema, R. Jinno, K. Nakayama, and J. van de Vis, arXiv:2102.12501 [hep-ph] [Search inSPIRE].
[62] T. Krajewski, K. Turzyński, and M. Wieczorek, Eur. Phys. J. C **79**, 654 (2019).
[63] O. Iarygina, E. I. Sfakianakis, D.-G. Wang, andA. J., Cosmol. Astropart. Phys. **06**, 027 (2019).
[64] O. Iarygina, E. I. Sfakianakis, D.-G. Wang, and A. Achúcarro, arXiv:2005.00528 [astro-ph.CO] [Search inSPIRE].
[65] G. Aad et al. Phys. Lett. B **796**, 68 (2019).
[66] A. M. Sirunyan et al. J. High Energy Phys. **07**, 208 (2021).
[67] M. H. Klein, PoS **ICHEP2020**, 064 (2021).
[68] G. Aad et al. Phys. Rev. D **101**, 012002 (2020).
[69] CMS Collaboration, CERN Report CMS-PAS-HIG-19-005 (2020).
[70] A. M. Sirunyan et al. Eur. Phys. J. C **79**, 421 (2019).
[71] T. Barklow, K. Fujii, S. Jung, R. Karl, J. List, T. Ogawa, M. E. Peskin, and J. Tian, Phys. Rev. D **97**, 053003 (2018).
[72] P. Bambade et al., arXiv:1903.01629 [hep-ex] [Search inSPIRE].
[73] R. Aaij et al. Phys. Rev. Lett. **124**, 041801 (2020).
[74] G. Salam and A. Weiler, Collider Reach (CERN, Geneva, 2021). (Available at: http://collider-reach.web.cern.ch/, date last accessed March 8, 2022).
[75] S. Jung and J. D. Wells, Phys. Rev. D **89**, 075004 (2014).
[76] G. Barenboim, E. J. Chun, S. Jung, and W. I. Park, Phys. Rev. D **90**, 035020 (2014).
[77] B. Batell and S. Jung, J. High Energy Phys. **07**, 061 (2015).
[78] A. D. Martin, W. J. Stirling, R. S. Thorne, and G. Watt, Eur. Phys. J. C **63**, 189 (2009).